Sādhanā Vol. 32, Parts 1 & 2, February–April 2007, pp. 65–81. © Printed in India

Some indications from instability results about the effectiveness of wall heating as a control option for channel flow

A SAMEEN† and RAMA GOVINDARAJAN

Engineering Mechanics Unit, Jawaharlal Nehru Centre for Advanced Scientific Research, Bangalore 560 064
†Present address: International Centre for Theoretical Physics, Trieste, Italy
e-mail: asameen@gmail.com; rama@jncasr.ac.in

Abstract. This paper is a review of some of our recent work on the effect of wall heating on the stability of laminar flow in a channel. The summary of our results, some of them unexpected, is as follows. Viscosity stratification has very little effect on transient growth, whereas it results in linear mode stabilising or destabilising by an order of magnitude. It has hitherto been accepted that heat diffusivity does not affect stability. This is however true only for linear instability, transient growth is affected by an order of magnitude. Unusually, the growth is spanwise-independent and not in the form of streamwise vortices. It is also shown that flow is destabilised by secondary modes as the viscosity ratio increases. However, the viscosity ratio has no role in the selection of the pattern of Λ vortices.

Keywords. Secondary instability; viscosity-stratification; heat diffusivity.

1. Background

Critical Reynolds number for linear instability in a plane Poiseuille flow is 5772·22 (Orszag 1971). However, experiments usually find fully developed turbulence at a much lower Reynolds number, around 1500. It is clear that alternative routes to turbulence are in operation. This work particularly deals with two of them: *secondary instabilities* of the stable primary modes and *algebraic growth*. Both these routes in channel flows can trigger transition at a Reynolds number lower than that for linear instability. The background noise in the flow has a major influence in delaying/hastening transition to turbulence, as well as in deciding which mechanism is dominant (Morkovin *et al* 1994; Reshotko 2001). At lower levels, a traditional TS mechanism and/or secondary instability is likely to be followed, whereas at fairly large noise levels transient growth is likely to occur, leading to "bypass" transition. Our interest is to explore the effect of large viscosity stratification on these mechanisms.

A linearly stable flow, i.e., one where all the TS modes are slowly decaying, can become unstable to secondary three-dimensional perturbations. This instability route is followed in a

channel for low to intermediate background noise (Huerre & Rossi 1998). Secondary instability analysis consists of looking for instabilities of a mean flow periodic in space and time. (The mean flow is now the sum of a steady laminar plane Poiseuille flow and a finite amplitude TS wave whose phase speed is c.)

The traditional TS route is often referred to as *natural transition* where the instability occurs in sequence from TS waves to three-dimensional secondary waves. However, as in pipe and plane channels, there are occasions when classical linear stability theory or even secondary instability fails to justify the early transitions found in experiments. An alternative mechanism was constantly being sought. In the last two decades of the 20th century (see Hultgren & Gustavsson, 1981 and Landahl 1980) transient growth analysis gained importance. The transient growth mechanism was first discovered by Ellingsen & Palm (1975) and Landahl (1980) as an inviscid mechanism of algebraic kinetic energy growth. The enlightening demonstration of Reddy *et al* (1993) and Trefethen *et al* (1993) that the non-normality of the linear stability operator can lead to algebraic growth even when the eigenmodes are decaying, led to a host of studies on transient growth in different flows (for example, Corbett & Bottaro 2001, Foster 1997, Meseguer 2002).

The crux of the analysis is in identifying the governing linear stability equations as an initial value problem. The subcritical transition observed may be attributed to the considerable amplification or transient growth of small perturbation due to the non-orthogonality of eigenvectors. Henningson (1988) showed that the algebraic instability is due to the generation of vertical vorticity through the coupling between Orr–Sommerfeld and Squire modes. The inclined shear layers thus formed intensify with time. This creates a weakly damped streamwise vortex, which advects fluid in the normal direction resulting in high and low speed longitudinal streaks. Landahl (1980) described this as the "lift-up" mechanism. Andersson *et al* (2001), Reddy *et al* (1998, 1993), Schmid & Henningson (2001) and Waleffe (1995a,b) go into detail about the streak and oblique transition possible in several kinds of flows. As streamwise vortices evolve with spanwise periodicity, the streamwise velocity profile $U(y, z)$ of the streaks attain inflexional points both in y and z directions leading to inflexional instability. In oblique transition, a pair of oblique waves interact nonlinearly to create streamwise-independent structures including streamwise vortices. The selection of the mode of instability mechanism largely depends on the initial amplitude of the wave.

Even though it is known that variable properties can alter flow-stability characteristics, the quantum of work on transition in these kind of flows is much less compared to constant property transition regimes. The effect of viscosity-stratification on *linear stability* seems to be the only situation studied by many researchers. Two related studies of transient growth had emphasis different from that of our work. Transient growth in two-fluid flow was studied in two-dimensions by Malik & Hooper (2005) with the objective of understanding the effect of the interface. Biau & Bottaro (2004) studied transient growth with stable thermal stratification and concluded that such stratification is a viable strategy to control transitional flows.

2. Basic velocity profiles

The two walls of the channel are maintained at different temperatures. Neglecting effects due to viscous dissipation in the energy equation, we obtain a linear temperature profile. The temperature-dependence of the viscosity is described by the Arrhenius model, which works fairly well for most common liquids like water and alcohol. The streamwise direction

is denoted as x, the coordinate y is normal to the wall, and z is the spanwise direction. The mean x-momentum equation for a plane parallel channel flow reduces to

$$(\mu U')' = \mathrm{d}P/\mathrm{d}x\ \mathrm{Re}, \tag{1}$$

where the primes denote differentiation with respect to y, Re is the Reynolds number defined as $\mathrm{Re} = U_{\max}h/\nu_{\mathrm{ref}}$, h is the half-channel width, ν_{ref} is the reference kinematic viscosity, and $\mathrm{d}P\mathrm{d}x$ is the constant pressure gradient. The viscosity ratio is defined as $m = \mu_{\mathrm{cold}}/\mu_{\mathrm{hot}}$. Knowing $\mu(T)$ and $T(y)$, (1) is integrated twice by a fourth-order Runge–Kutta method to get U.

3. Linear stability analysis

The disturbance quantities in normal mode form are given as

$$[\hat{v}, \hat{\eta}, \tilde{T}] = [v(y), \eta(y), \hat{T}(y)] \exp[i(\alpha x + \beta z - \omega t)], \tag{2}$$

where $\hat{v}$ and $\hat{\eta}$ respectively are the components of disturbance velocity and vorticity in the direction normal to the wall, $\tilde{T}$ is the disturbance temperature, α and β are the wave numbers in the streamwise and spanwise directions respectively, and ω is the complex frequency of the wave. The linear stability equations may be derived to be (Sameen & Govindarajan 2007; Wall & Wilson 1996)

$$\begin{aligned} &i\alpha[(v'' - (\alpha^2+\beta^2))(U-c) - U''v] \\ &\quad = \frac{1}{\mathrm{Re}}\Big[\mu[v^{iv} - 2(\alpha^2+\beta^2)v'' + (\alpha^2+\beta^2)^2 v] \\ &\qquad + \frac{\mathrm{d}\mu}{\mathrm{d}T}T'2[v''' - (\alpha^2+\beta^2)v'] + \frac{\mathrm{d}\mu}{\mathrm{d}T}T''[v'' + (\alpha^2+\beta^2)v] \\ &\qquad + \frac{\mathrm{d}^2\mu}{\mathrm{d}T^2}T''[v'' + (\alpha^2+\beta^2)v] + \frac{\mathrm{d}\mu}{\mathrm{d}T}[U'\hat{T}'' + 2U''\hat{T}' + (\alpha^2 U' + U''')\hat{T}] \\ &\qquad + 2\frac{\mathrm{d}^2\mu}{\mathrm{d}T^2}U'T'\hat{T}' + \frac{\mathrm{d}^2\mu}{\mathrm{d}T^2}T''U'\hat{T} + \frac{\mathrm{d}^3\mu}{\mathrm{d}T^3}U'T'\hat{T}\Big], \end{aligned} \tag{3}$$

$$\begin{aligned} &i\alpha(U-c)\eta + i\beta U'v \\ &\quad = \frac{1}{\mathrm{Re}}\Big[\mu[\eta'' - (\alpha^2+\beta^2)\eta] + \frac{\mathrm{d}\mu}{\mathrm{d}T}T'\eta' \\ &\qquad - i\beta\frac{\mathrm{d}\mu}{\mathrm{d}T}(U''\hat{T} + U'\hat{T}') - i\frac{\mathrm{d}^2\mu}{\mathrm{d}T^2}T'U'\hat{T}\Big], \end{aligned} \tag{4}$$

$$i\alpha(U-c)\hat{T} + T'v = \frac{1}{\mathrm{RePr}}[\hat{T}'' - (\alpha^2+\beta^2)\hat{T}], \tag{5}$$

where $c \equiv \omega/\alpha$. Equations 3 and 4 respectively are the Orr–Sommerfeld and Squires equations, modified here to account for the effects of viscosity variations, temperature fluctuations.

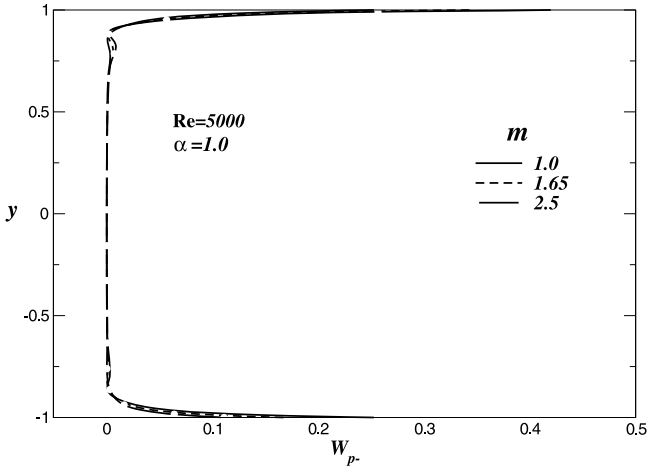

Figure 1. The kinetic energy dissipation for various viscosity ratios, Re = 5000 and $\alpha = 1{\cdot}0$.

In order to isolate the effect of viscosity variation, the Prandtl number is first set to zero. We plot the kinetic energy dissipation and production (Govindarajan *et al* 2003) for various viscosity ratios in figures 1 and 2. The critical Reynolds numbers are shown in figure 3. As viscosity ratio increases, the flow becomes stable. We define the Reynolds number in terms of average viscosity, and compare results at a given Reynolds number.

We know that for liquids such as water, heat diffuses slower than momentum, so the assumption of $\mathrm{Pr} = 0$ is not justifiable. Surprisingly, however, the linear stability, as measured by the least stable eigenmode, is practically unaffected by a decrease in heat diffusivity (Wall & Wilson 1996). Present computations confirm this (figure 4). However, the prevalent conclusion that heat diffusivity does not affect flow stability, and therefore that the Peclet number may be set to zero in stability analyses, is incorrect. Increasing the Prandtl number to $O(1)$ values can enhance transient growth by an order of magnitude, as seen in the next section.

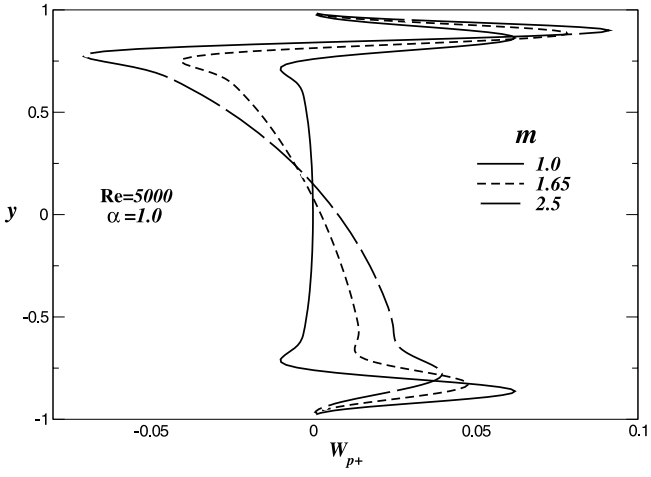

Figure 2. The kinetic energy production for various viscosity ratios, Re = 5000 and $\alpha = 1{\cdot}0$.

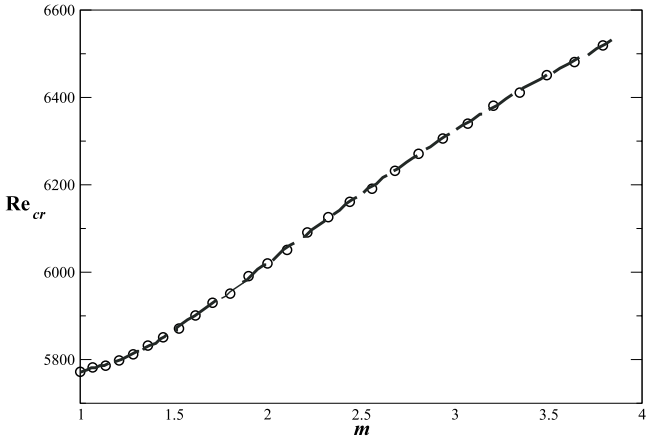

Figure 3. Effect of viscosity variation on linear stability. For unstratified flow, i.e., at $m = 1{\cdot}0$, Re_{cr} is 5772·2.

4. Transient growth

The linear stability operator is not self-adjoint, and the resulting non-orthogonality of the eigenfunctions is known to be able to give rise to large levels of transient growth of disturbance kinetic energy even when all individual eigenmodes are stable. In wall-bounded flows, transient growth is mainly caused by the interaction between the Orr–Sommerfeld and Squire modes (Criminale *et al* 2003; Reddy & Henningson 1993) from the coupling term, $-i\beta U'$, appearing in Squire's equation. In the presence of a temperature gradient, at non-zero Prandtl numbers, there is an additional coupling term $T'v$ which can cause transient growth. Mathematically, the role of this term is similar to the Squire modes mentioned above. Its actual contribution to the transient growth is discussed below and in Sameen & Govindarajan (2007). In constant temperature flows, the most likely structures arising due to transient growth are streamwise streaks (Reddy & Henningson 1993, 1994; Reddy *et al* 1998; Schmid & Henningson 2001). However, in the present case, at higher Prandtl numbers the most preferred structures are spanwise independent. We use the standard approach for

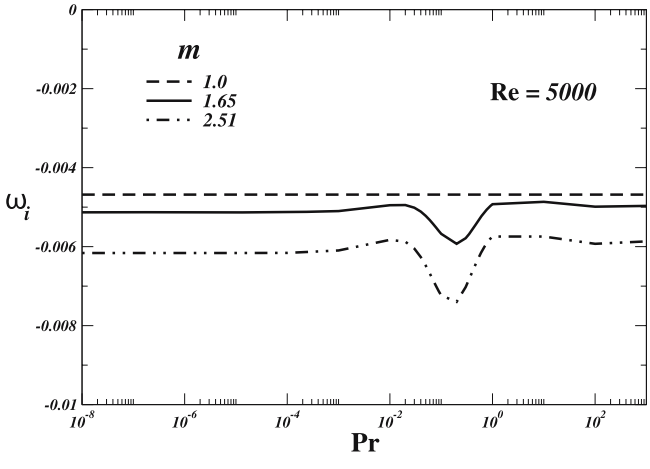

Figure 4. Most unstable eigenvalue at various Prandtl numbers for different ΔT at $\alpha = 0{\cdot}9$ and $\mathrm{Re} = 5000$. The effect of Prandtl number is negligible.

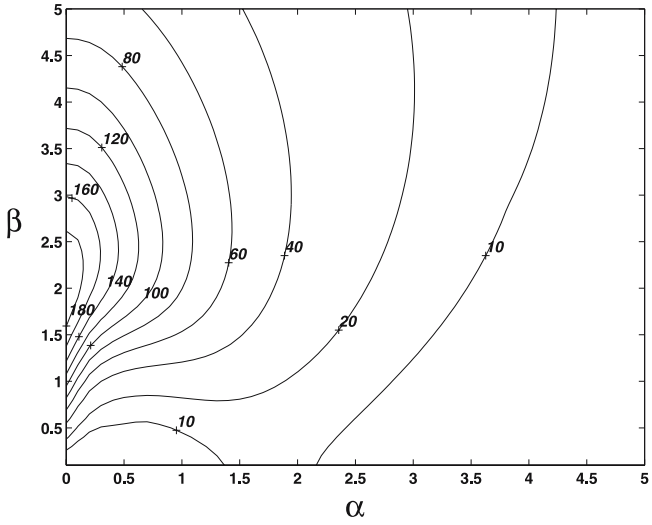

Figure 5. The contour of $G_{\max}$ (the maximum over time of $G(t)$) for Re $=$ 1000 in the $\alpha - \beta$ plane, $\Delta T = 0$K. This matches well with Reddy & Henningson (1993).

computing the maximum transient growth. The basic idea is sketched in the appendix, where the quantity $G(t)$ is defined. $G(t)$ is the largest factor over which the disturbance energy can grow algebraically, for the "worst case" (or best case, depending on whether we want transition to turbulence to take place or not) combination of initial amplitudes of different eigenmodes. We then define $G_{\max}$ as the maximum over time of $G(t)$ for one particular Re, α and ΔT.

The contour plot for $G_{\max}$ for unheated flow is shown at Re $=$ 1000 in figure 5, for comparison with the results for heated flow to follow. A maximum growth of $G_{\max} = 196$ is obtained for $\alpha = 0{\cdot}0$ and $\beta = 2{\cdot}05$ (see Reddy & Henningson 1993).

The effect of viscosity stratification, in contexts other than heat (Chikkadi *et al* 2005; Malik & Hooper 2005) has been addressed earlier, though not completely. The effect of buoyancy has been studied under stable stratification alone by Biau & Bottaro (2004). The effect of heat diffusivity on transient growth has not been studied by others, to our knowledge.

4.1 *Effect of viscosity stratification*

As before, we first take the Prandtl number to be zero, i.e., assume that temperature fluctuations diffuse away instantaneously. The effect of asymmetric heating is quantified in figure 6 in terms of $G_{\max}$ at $\alpha = 0$ and $\beta = 2$. There is a marginal stabilisation with viscosity stratification. This result is in line with the result for linear stability, but much smaller in magnitude.

The insignificant effect of viscosity stratification is consistent with our recent study of transient growth in two-fluid and non-Newtonian flows (Chikkadi *et al* 2005). As discussed there, the U'' term, which affects the least stable eigenmode dramatically, has no effect on streamwise vortices arising from $\alpha = 0$, which dictates transient growth.

4.2 *Effect of heat diffusivity*

It has been seen that the Prandtl number has a marginal effect on the most unstable linear mode. In contrast, we find here that reducing heat diffusivity has a large destabilising effect

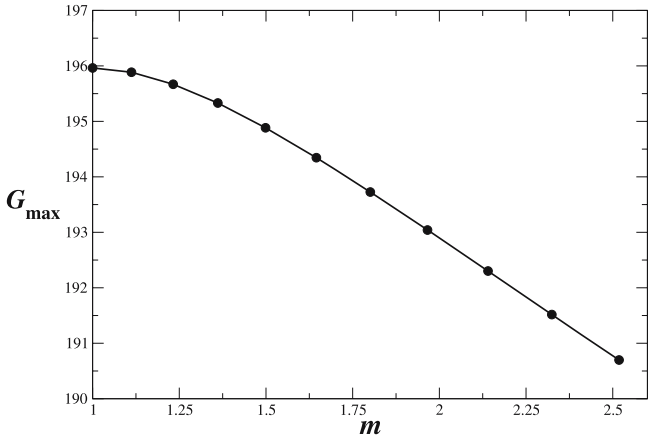

Figure 6. The variation of $G_{\max}$ at $\alpha = 0$ and $\beta = 2$ for various viscosity ratios at Re $= 1000$, asymmetric heating. The maximum deviation of $G_{\max}$ from the unheated value of 196 is only 3% (Sameen & Govindarajan (2007).

on the transient growth of disturbance kinetic energy. A dimensionless quantity for measuring growth is the energy norm (see appendix A for details) defined as,

$$E = \int |u|^2 + |v|^2 + |w|^2 + |\hat{T}|^2 \mathrm{d}y. \tag{6}$$

There is some flexibility in defining the measure, but the results are not expected to change qualitatively (Biau & Bottaro 2004; Hanifi & Henningson 1998). This point, and the effect of the temperature perturbations on transient growth, is discussed in some detail by Sameen & Govindarajan (2007). In figure 7 for a temperature difference of 25K at a Reynolds number of 1000, the effect of Prandtl number is shown. As the Prandtl number is increased from 10^{-4} to 1, the transient growth is seen to increase dramatically. The large destabilisation comes from a new two-dimensional transient growth. This is true for symmetric heating as well (not shown). We now have a situation where transient growth dominates, but not via the standard streamwise streaks and streamwise vortices.

According to the present wisdom on which route to transition is preferred in a given case, if the background turbulence and other disturbances in a channel flow are extremely small, the linear instability route is taken (Nishioka *et al* 1975). At somewhat higher but still very low levels of disturbance, the least stable linear modes at Reynolds numbers below the critical are possibly dominant over the others, and can give rise to secondary modes of instability, as described in the following section. If, however, the background turbulence is moderately high, several decaying linear modes, as seen above, can interact to give rise to levels of algebraic growth sufficient to trigger nonlinearity.

5. Secondary instability analysis

Primary instability analysis gives an indication of the modal growth or decay. In many cases the TS waves may not decay and may form a more complicated mean flow. The new mean flows are often unstable to infinitesimal disturbances. The technique to approximate the nonlinear effects or small finite amplitude effects using secondary instability analysis is to add infinitesimal perturbations in succession and linearise the system of equations. In channel

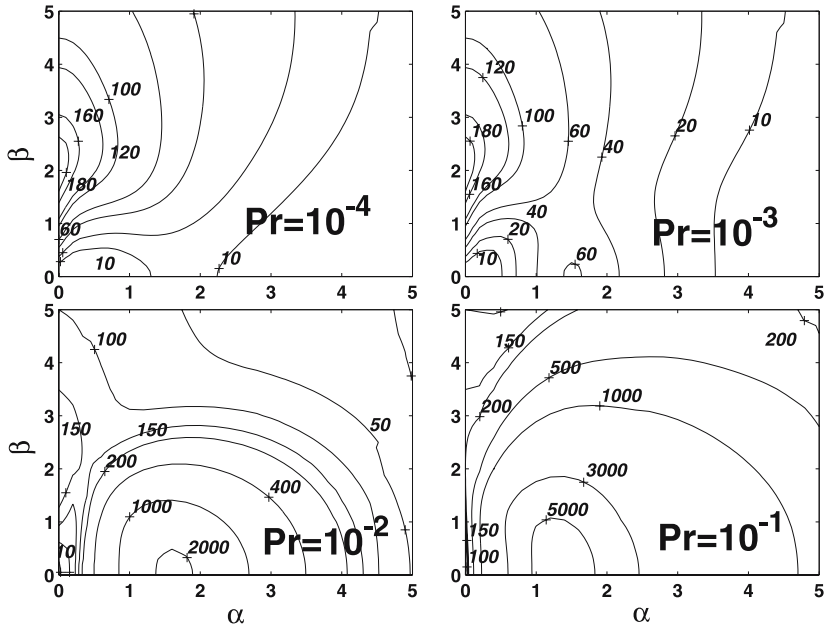

Figure 7. Contour plot of $G_{\max}$ for $T = 25$K, Re $= 1000$ for various Prandtl numbers.

flow, even in primary mode decays, new disturbances can superpose to form a secondary disturbance. The most unstable mode is usually followed in secondary instability analysis. This is the secondary instability analysis in a nutshell.

The method here is as in Herbert (1983) and Bayly *et al* (1988). All flow variables are decomposed in the form

$$u = \bar{u} + A_p(\hat{u}_p) + A_s\hat{u}_s, \tag{7}$$

where $\bar{u}$ comes from the basic flow, $\hat{u}_p$ is the solution from linear stability analysis and $\hat{u}_s$ is the secondary instability solution that we seek. The direct interactions between primary instability are negligible, which means A_p^2 terms are neglected (also means $A_p^2 \ll A_pU, A_p\partial u/\partial y$). Assuming $1 \gg A_p > A_s$, we get a linear system of partial differential equations,

$$\mathcal{L}(u) = 0, \tag{8}$$

whose coefficients contain periodic functions of t. The secondary and primary waves have a phase difference. The difference in frequency between the two is often called a *frequency shift*. Herbert (1983) showed that for a subharmonic mode, the frequency shift vanishes for high values of β suggesting a *phase lock*. The growth rate is highly sensitive to the TS amplitude level, A_p. The amplitude at which the growth rate become positive is termed as the critical threshold amplitude. In Craik's mechanism this instability is possible at very low amplitude for boundary layers which is absent in channel flow because of symmetry of the flow geometry (Herbert & Morkovin 1980). The fundamental mode behaves similar to subharmonic modes, but the unstable modes are phase-locked with the primary. At low A_p, it is to be noted that secondary modes are all stable, while at high A_p both fundamental and subharmonic modes are unstable and highly dependent on initial perturbation. At some intermediate amplitude level, subharmonics are the most dominant mode.

The secondary perturbation quantities are three-dimensional and are assumed to be of the form

$$(\hat{u}_s, \hat{v}_s, \hat{w}_s) = \frac{1}{2}[(u_+, v_+, w_+)(y,t)e^{i(\alpha_+ x+\beta z)} + (u_-, v_-, w_-)(y,t)e^{i(\alpha_- x-\beta z)} + \text{c.c.}], \tag{9}$$

where α_+ and α_- are the wave numbers of the secondary waves in the streamwise direction, β is the wave number in the spanwise direction. The direct interaction between primary waves is assumed to be negligible, so the primary waves are,

$$\{\hat{u}_p; \hat{v}_p\} = \frac{1}{2}[\{u_p; v_p(y,t)\}e^{i\alpha_p x} + \text{c.c.}]. \tag{10}$$

For the flow under consideration, the growth/decay rates are so small that dA_p/dt can be neglected during one period of time. For $\omega_i \ll \omega_r$, the primary flow may thus be taken to be periodic. The most unstable primary mode alone is considered for the secondary instability analysis. Here we use Squire's theorem, namely that the two-dimensional wave becomes more unstable at lower Reynolds number than its three-dimensional counterpart. Substituting these decompositions in the three momentum equations, eliminating pressure and neglecting nonlinear terms in the secondary disturbance, we arrive at the secondary disturbance equation. On averaging over x, z and t, all terms become zero except the resonant modes, given by,

$$\alpha_+ + \alpha_- = \alpha. \tag{11}$$

Using the continuity equation, the streamwise component of secondary velocity is eliminated and we get the secondary perturbation equation.

$$-D\frac{\partial v_+}{\partial t} + s\frac{\partial f_+}{\partial t} = -sAf_+ + (AD - i\alpha_+(DU))v_+ - A_p\left[\frac{i\alpha_+^2}{2\alpha_-}u_p D + \frac{v_p\alpha_+ D^2}{2\alpha_-} + \frac{i(Du_p)\alpha_+}{2}\right]v_-^* + \frac{A_p\alpha_+^2}{2}\left[-v_p D + i\alpha_- u_p + \frac{i\beta_s^2}{\alpha_-}u_p + \frac{\beta_s^2}{\alpha_+\alpha_-}v_p D\right]f_-^*, \tag{12}$$

$$\frac{\partial v_+}{\partial t} - D\frac{\partial f_+}{\partial t} = -Av_+ + (AD + (DA))f_+ - \frac{A_p(\alpha+\alpha_-)}{2}\left[\frac{v_p}{\alpha_-}D - iu_p\right]v_-^* + \frac{A_p}{2}\left[-i(\alpha+\alpha_-)u_p D - i\alpha_-(Du_p) + v_p\left(\frac{\alpha_+\beta_s^2}{\alpha_-} + D^2\right)\right]f_-^*, \tag{13}$$

where $A = [i\alpha_+ U + \mu s - \mu d^2 - \mu' D]$, $f_+ = -(i/\beta_s)w_+$, $s = \alpha_+^2 + \beta_s^2$, $D = d/dy$. Equations (12) and (13) and their complementary equations for v_-^* and f_-^* are solved using Chebyshev collocation spectral methods, with the boundary conditions $\hat{u}_s, \hat{v}_s, \hat{w}_s = 0$ at $y = \pm 1$. The dispersion relation is $F(A_p, \beta, m, \text{Re}, \alpha, c,) = 0$ (see Herbert 1983).

5.1 *Method of solution*

The formulation described in the above section leads to an eigenvalue problem. The set of perturbation equations, along with the corresponding boundary conditions, form the complete eigenvalue problem after discretisation. A temporal analysis is done here. The form of the discretised equations is given below.

$$\begin{bmatrix} A_{11} & A_{12} & A_{13} & A_{14} \\ A_{21} & A_{22} & A_{23} & A_{24} \\ A_{31} & A_{32} & A_{33} & A_{34} \\ A_{41} & A_{42} & A_{43} & A_{44} \end{bmatrix} \begin{bmatrix} v_+ \\ f_+ \\ v_-^* \\ f_-^* \end{bmatrix} = -i\omega_s \begin{bmatrix} B_{11} & B_{12} & B_{13} & B_{14} \\ B_{21} & B_{22} & B_{23} & B_{24} \\ B_{31} & B_{32} & B_{33} & B_{34} \\ B_{41} & B_{42} & B_{43} & B_{44} \end{bmatrix} \begin{bmatrix} v_+ \\ f_+ \\ v_-^* \\ f_-^* \end{bmatrix}. \quad (14)$$

Equation (14) can be solved using any of the standard packages available, e.g. LAPACK library functions. The results are discussed in the section that follows.

The first step is to find the effect of A_p on the secondary growth rate ω_{is}. The figure 8 shows the dependence of the growth rate on A_p. Here we neglect the time-dependence of the amplitude of the primary mode. The growth rate of the secondary mode is computed for a periodic primary mode. The secondary growth rate is a function of the primary amplitude (which decays very slowly in time). At low A_p, all the secondary modes are stable. Huerre & Rossi (1998) argue from experiments of Klebanoff *et al* (1962) and Kozlov & Ramazanov (1984) that for large A_p the unstable modes can be both fundamental and subharmonic, but at some intermediate A_p the subharmonic mode is essentially the dominating one. It is shown in this section that for intermediate A_p, the most unstable mode can be either fundamental or subharmonic depending on the value of spanwise and streamwise wave numbers. A value of $A_p = 0{\cdot}01$ is taken to be representative of an intermediate level of primary disturbance. Figure 8 also shows that the growth rate behaviour for various viscosity ratios is similar. The curves deviate from one another only for very large A_p.

A secondary amplitude level A_s can be computed as a multiple of its initial value. We compute the secondary growth rate at a given time considering the primary to be strictly periodic. In fact the primary amplitude, $A_p(t)$, is a slowly decaying function of time. Integrating instantaneous results over long time periods, we can compute the time-dependence

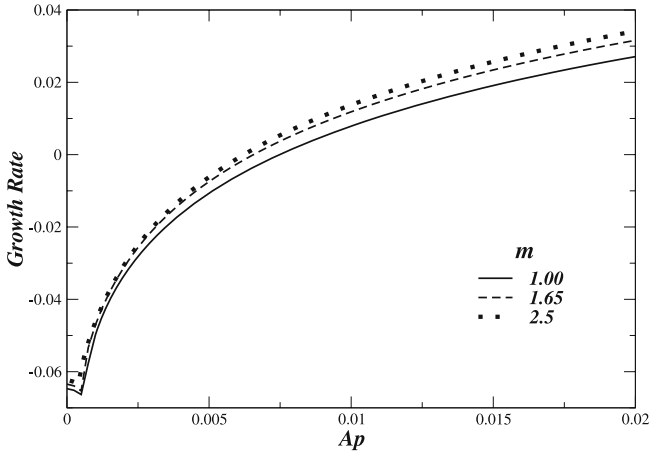

Figure 8. The growth rate variation with A_p for various viscosity ratios. $\alpha = 1{\cdot}0$, $\beta = 2{\cdot}0$, Re $=$ 5000, Subharmonic mode.

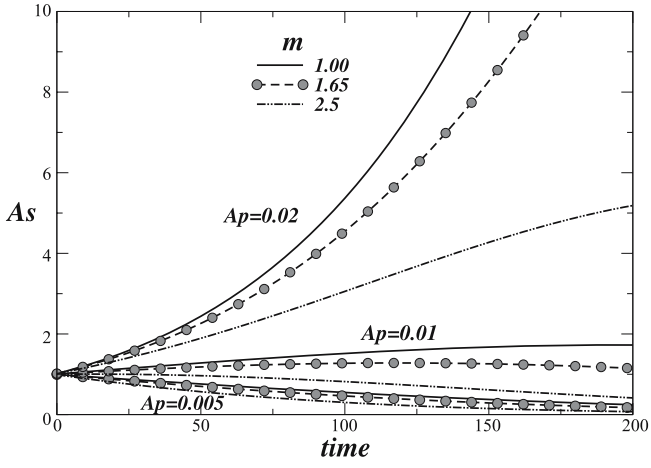

Figure 9. Amplitude variation in time of secondary disturbance for three sets of initial A_p. $\alpha = 1{\cdot}0, \beta = 0{\cdot}5, \mathrm{Re} = 5000$, Subharmonic mode.

of amplitude of secondary mode. This is a time counterpart of the parallel flow assumption in slowly x-varying flows. The amplitude of the secondary mode A_s is shown as a function of time in figure 9. At low initial A_p the secondary modes are always stable while for higher A_p the mode catastrophically grows. For some intermediate A_p growth or decay depends on spanwise wave number. The growths shown in the above two figures are for subharmonic secondary waves. For $\beta = 0{\cdot}5$, the effect of small viscosity ratio is stabilising. But for $\beta = 2{\cdot}0$ the effect is reversed.

The variation of secondary growth rate with the spanwise wave number for various viscosity ratios is plotted in figure 10. For a non-zero temperature difference, a second mode appears, which does not exist in unstratified flow. This second mode is highly unstable, compared to the usual unstratified mode. Another interesting feature to note is the stabilizing effect of temperature difference for low wave numbers. At the point from where the new mode dominates, the secondary wave has no phase shift from the primary wave.

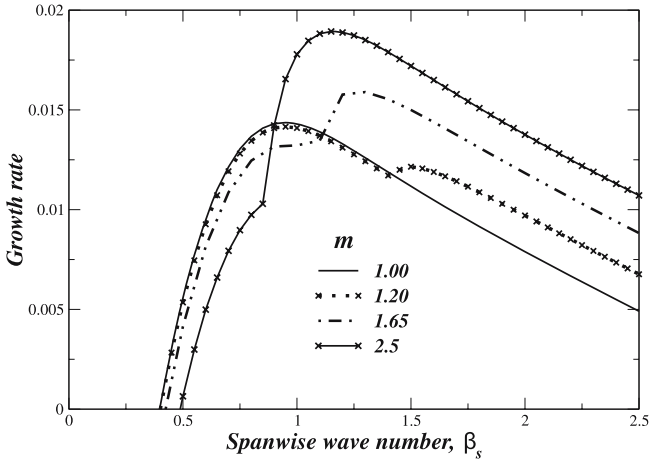

Figure 10. The dependence of growth rate on spanwise wave number of the secondary disturbance for various viscosity ratios, subharmonic case. $\alpha = 1{\cdot}0, A_p = 0{\cdot}01$, Re = 5000 Sameen & Govindarajan (2007).

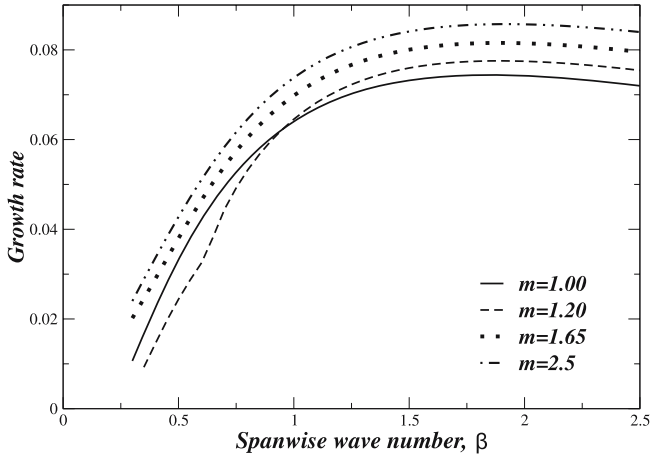

Figure 11. Same as figure 10 except that $\alpha = 2{\cdot}0$. For a large α second mode dominates.

The new second mode dominates for a higher streamwise primary wave number, α as shown in figure 11. It is to be noted that at this α, the primary wave is highly damped, and therefore this mode occurs only for background noise of special spectral content.

6. Secondary critical points

We now plot the "neutral stability curve" for the secondary instability. The secondary wave is chosen to be subharmonic. For various obliqueness β of the secondary wave, the neutral curve is plotted as in figure 12. The A_p is fixed at $0{\cdot}01$ for all the β. This is performed for various viscosity ratios. As can be seen from figures 12, 13 and 14, as the obliqueness increases, the flow becomes more and more unstable and after some β the trend reverses. (If the obliqueness increases more than a certain value, then resonance of secondary and primary wave will be weakened. This could be the reason for the stabilising effect at high β.) Another conspicuous fact from these figures is a second new mode of eigenvalue for viscosity stratified cases. As

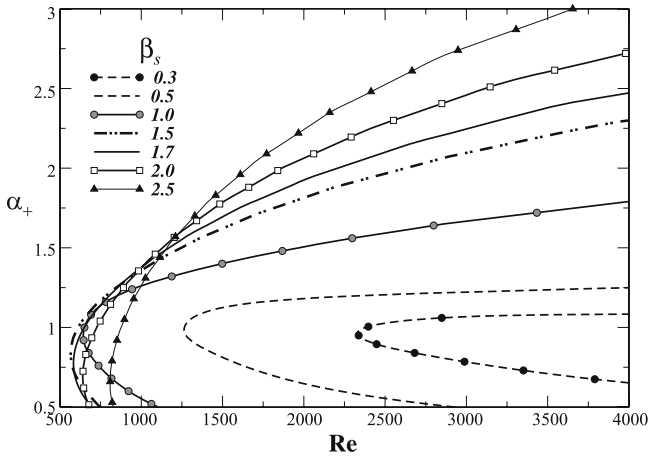

Figure 12. The "neutral" curves for secondary instability for various spanwise wave numbers, β, for subharmonic modes for $m = 1{\cdot}0$ and $A_p = 0{\cdot}01$.

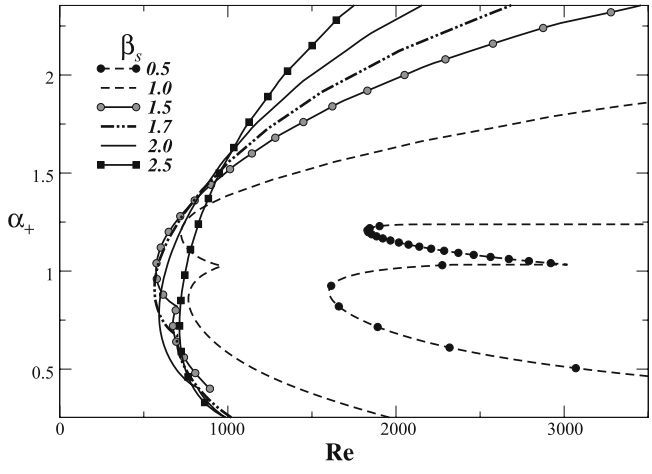

Figure 13. The "neutral" curves for secondary instability for various spanwise wave numbers, β, for subharmonic modes for $m = 1{\cdot}65$ and $A_p = 0{\cdot}01$.

explained in the previous section, these modes are the dominating ones at large β values. These modes also point to a possible "double critical value" for stratified cases.

7. Λ Vortices

Λ vortices form a pattern of growing secondary modes due to the alternating 'peak' and 'valleys' in the spanwise direction. These are regions of the enhanced and reduced disturbance amplitudes of the mean longitudinal vortex system (Herbert 1983). If the secondary wave is a harmonic of the primary wave, the resulting Λ structures are called Klebanoff (aligned) type, and if subharmonic they are called Herbert (staggered) type. In the exercise that follows, the primary wave number α is kept constant at some value. The secondary wave number α_+ is varied for a given β, and the α_+ corresponding to the most unstable mode is plotted in the y-axis against the corresponding β. These are plotted in figure 15.

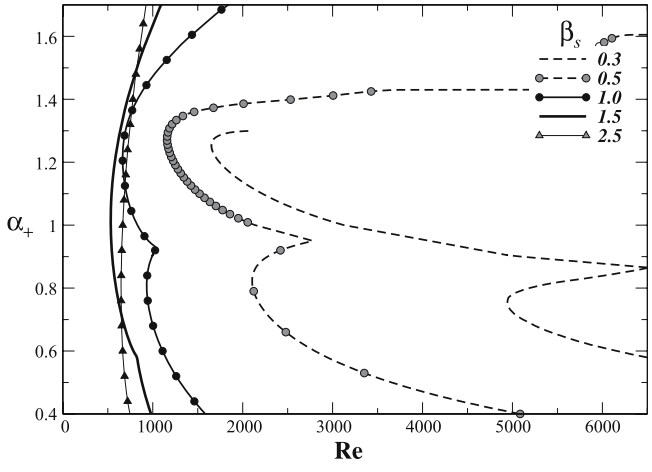

Figure 14. The "neutral" curves for secondary instability for various spanwise wave numbers, β, for subharmonic modes for $m = 2{\cdot}5$ and $A_p = 0{\cdot}01$.

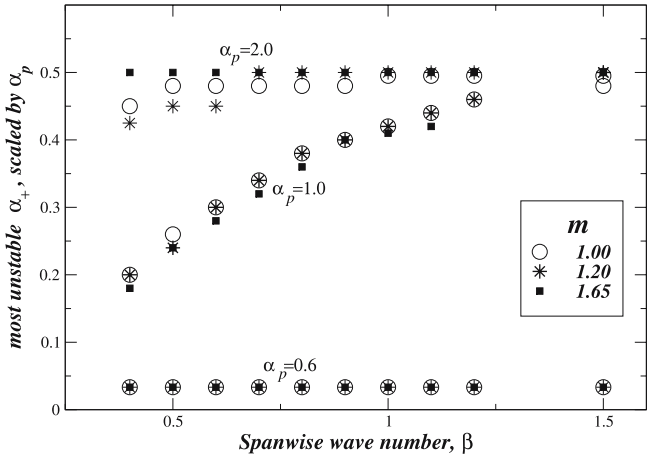

Figure 15. The most unstable α_+ scaled by corresponding α against β for various viscosity ratios. $A_p = 0{\cdot}01$, Re $= 5000$.

Figure 15 plots the most unstable α_+ for various cases of α_p. Each α_+ is scaled by the corresponding α_p. For high α_p the second mode (which is subharmonic) is dominating, consistent with figures 10 and 11. Figure 15 shows that the subharmonic mode is more unstable at higher wave numbers while the flow is unstable due to the Klebanoff mode at lower wave numbers. This is expected, since the chances for the secondary wave to be in phase with the primary are more if the obliqueness of the wave is less. But what is more interesting is that this behaviour does not change for different temperature gradients (viscosity ratios). We may conclude that the viscosity variation has no role to play in the selection of Herbert or Klebanoff mode. The experiment is repeated for various α_p. Further, from figure 16, it can be concluded that the effect of Reynolds number on this selection is marginal.

8. Conclusion

Control of flow using heating or cooling of the surface has long been practised, especially in open flows. In plane channel flow, we have conducted a comprehensive study of the effect of

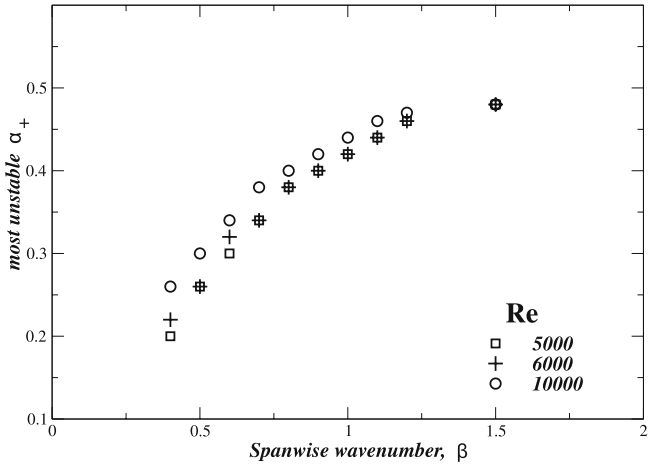

Figure 16. For unstratified flow ($m = 1{\cdot}0$) the most unstable α_+ against β for various Re. $\alpha_p = 1{\cdot}0$, $A_p = 0{\cdot}01$.

heat. Linear stability results are consistent with earlier studies in that the most unstable linear mode is suppressed when viscosity decreases towards the wall. Also the effect of Prandtl number is negligible.

The transient growth of disturbances is unaffected by viscosity stratification, but hugely increased by reduced heat diffusivity. Both of these are counter to the effect on the least stable linear mode. The Prandtl number is thus not an unimportant parameter, as was hitherto assumed. Although the effect of buoyancy has not been discussed here, we mention that transient growth is also very high in the presence of buoyancy of the appropriate sign. With increasing Prandtl number, the growth is two-dimensional, not in streamwise streaks, which is quite unusual for transient growth.

It is a pleasure to dedicate this paper to Dr P R Viswanath. RG would like to thank him for constant encouragement through the years in NAL and later.

Appendix A. Computation of maximum transient growth

We discuss the transient algebraic evolution of linear perturbations. The methodology is the same as used in Schmid & Henningson (2001), Reddy & Henningson (1993) or Meseguer (2002). Consider the linear sub-space S_N spanned by the first N most unstable eigenvalues $\{\omega_1, \omega_2, \ldots \omega_N\}$ of the spectrum of equations (3) to (5).

$$S_N = \langle v_{p1}, v_{p2}, \ldots, v_{pN} \rangle, \tag{A1}$$

where v_{pi} is the ith eigenvector. A linear combination of v_{pi} can sum up to a perturbation quantity $\hat{v}_p$, such as

$$\begin{aligned} \hat{v}_p(y,t) &= \sum_{j=1}^{N} \kappa_j(0) e^{-i\Lambda t} v_p(y) \\ &= \sum_{j=1}^{N} \kappa_j(t) v_p(y), \end{aligned} \tag{A2}$$

where κ_j is the jth expansion coefficient of the eigenfunction and its time evolution is represented by the matrix

$$\partial\kappa/\partial t = -i\Lambda\kappa, \tag{A3}$$

where $\kappa = (\kappa_1, \kappa_2, \ldots, \kappa_N)^T$ and $\Lambda = \mathrm{diag}\{\omega_1, \omega_2, \ldots \omega_N\}$. The superscript T denotes the transpose operation.

A matrix of inner products between eigenvectors may be constructed as

$$\mathcal{M} = (v_{pi}, v_{pj})_E = \|v_p\|_E^2. \tag{A4}$$

The subscript E denotes the energy. This is a positive definite matrix which may be decomposed in the form $\mathcal{M} = \mathcal{F}^\dagger \mathcal{F}$, where $\dagger$ stands for the Hermitian conjugate. The energy norm of the perturbation is defined by the inner product

$$\varepsilon(\hat{v}_p) = (\hat{v}_p, \hat{v}_p)_E = \int_{-1}^{+1} (\hat{v}_p^* \cdot \hat{v}_p) \mathrm{d}y. \tag{A5}$$

Using (A4) the energy norm (A5) can be expressed as

$$\varepsilon(\hat{v}_p) = \|\kappa\|_E^2 = (\kappa, \kappa)_E$$
$$= (\mathcal{F}\kappa, \mathcal{F}\kappa)_2 = \|\mathcal{F}\kappa\|_2^2. \tag{A6}$$

Now, we define energy, $g(t)$ (Schmid & Henningson 2001), for an initial condition $\kappa(0)$ as,

$$g(t) = \frac{\|\kappa(t)\|_E^2}{\|\kappa(0)\|_E^2} = \frac{\|e^{-i\Lambda t}\kappa(0)\|_E^2}{\|\kappa(0)\|_E^2}. \tag{A7}$$

Maximising (A7) for all possible initial conditions $\kappa(0)$,

$$G(t) = \max_{\kappa\neq 0} g(t) = \max_{k\neq 0} \frac{\|e^{-i\Lambda t}\kappa(0)\|_E^2}{\|\kappa(0)\|_E^2}$$
$$= \max_{k\neq 0} \frac{\|\mathcal{F}e^{-i\Lambda t}\kappa(0)\|_2^2}{\|\mathcal{F}\kappa(0)\|_2^2}$$
$$= \|\mathcal{F}e^{-i\Lambda t}\mathcal{F}^{-1}\|_2^2. \tag{A8}$$

We define $G_{\max}$ as the maximum of $G(t)$ for one particular Re, α_p and m.

References

Andersson P, Brandt L, Bottaro A, Henningson D S 2001 On the breakdown of boundary layer streaks. *J. Fluid Mech.* 428: 29–60

Bayly B J, Orszag S A, Herbert T 1988 Instability mechanisms in shear-flow transition. *Annu. Rev. Fluid Mech.* 20: 359–391

Biau D, Bottaro A 2004 The effect of stable thermal stratification on shear flow instability. *Phys. Fluids* 16: 4742–4745

Chikkadi V K, Sameen A, Govindarajan R 2005 Preventing transition to turbulence: viscosity stratification will not always help. *Phys. Rev. Lett.* 95: 264504

Corbett P, Bottaro A 2001 Optimal linear growth in swept boundary layers. *J. Fluid Mech.* 435: 1–23

Criminale W O, Jackson T L, Joslin R D 2003 *Theory and computation in hydrodynamic stability* (Cambridge: University Press)

Ellingsen T, Palm E 1975 Stability of linear flow. *Phys. Fluids* 18: 487

Foster R 1997 Structure and energetics of optimal Ekman layer perturbations. *J. Fluid Mech.* 333: 97–123

Govindarajan R, L'vov, S V, Procaccia I, Sameen A 2003 Stabilization of hydrodynamic flows by small viscosity variations. *Phys. Rev.* E67: 026310

Hanifi A, Henningson D S 1998 The compressible inviscid algebraic instability for streamwise independent disturbances. *Phys. Fluids* 10: 1784

Henningson D S 1988 The inviscid initial value problem for a piecewise linear mean flow. *Stud. Appl. Math.* 78: 31

Herbert T 1983 Secondary instability of plane channel flow to subharmonic three-dimensional disturbances. *Phys. Fluids* 26: 871–874

Herbert T, Morkovin M V 1980 In *Laminar-turbulent transition* (ed.) R Eppler, H Fasel (Berlin: Springer-Verlag)

Huerre P, Rossi M 1998 Hydrodynamic instabilities in openflows. In *Hydrodynamics and nonlinear instabilities* (eds) C Godreche, P Manneville (Cambridge: University Press) pp 81–288

Hultgren L S, Gustavsson H L 1981 Algebraic growth of disturbance in a laminar boundary. *Phys. Fluids* 24: 1000–1004

Klebanoff P S, Tidstrom K D, Sargent L M 1962 The three-dimensional nature of boundary-layer instability. *J. Fluid Mech.* 12: 1–34

Kozlov V V, Ramazanov M P 1984 Development of finite-amplitude disturbance in Poiseuille flow. *J. Fluid Mech.* 147: 149–157

Landahl M T 1980 A note on an algebraic instability of inviscid parallel shear flows. *J. Fluid Mech.* 98: 243–251

Malik V S, Hooper P A 2005 Linear stability and energy growth of viscosity stratified flows. *Phys. Fluids* 17: 024101

Meseguer, A 2002 Energy transient growth in the Taylor–Couette problem. *Phys. Fluids* 14:

Morkovin M V, Roshotko E, Herbert T 1994 Transition in open flow systems – a reassessment. *Bull. Am. Phys. Soc.* 39: 1882

Nishioka M, Iida S, Ichikawa Y 1975 An experimental investigation of the stability of plane Poiseuille flow. *J. Fluid Mech.* 72: 731–751

Orszag S A 1971 Accurate solution of the Orr–Sommerfeld stability equation. *J. Fluid Mech.* 50: 689–703

Reddy S C, Henningson D S 1993 Energy growth in viscous channel flows. *J. Fluid Mech.* 252: 209–238

Reddy S C, Henningson D S 1994 On the role of linear mechanisms in transition to turbulence. *Phys. Fluids* 6: 1396

Reddy S C, Schmid P J, Bagget J S, Henningson D S 1998 On stability of streamwise streaks and transition thresholds in plane channel flows. *J. Fluid Mech.* 365: 269–303

Reddy S C, Schmid P J, Henningson D S 1993 Pseudospectra of the Orr–Sommerfeld operator. *SIAM J. Appl. Math.* 53: 1000–1004

Reshotko E 2001 Transient growth: A factor in bypass transition. *Phys. Fluids* 13: 1067

Sameen A 2004 *Stability of plane channel flow with viscosity-stratification*. Ph D thesis, Dept. of Aerospace Engineering, Indian Institute of Science, Bangalore

Sameen A, Govindarajan R 2007 The effect of wall heating on instability of channel flow. *J. Fluid Mech.* 577: 417–442

Schmid P J, Henningson D S 2001 *Stability and transition in shear flows* (New York: Springer-Verlag)

Trefethen L N, Trefethen A E, Reddy S C, Driscoll T A 1993 Hydrodynamic stability without eigenvalues. *Science* 261: 578

Waleffe F 1995a Hydrodynamic stability and turbulence: Beyond transients to a self-sustaining process. *Stud. Appl. Math.* 95: 319–343

Waleffe F 1995b Transition in shear flows. Nonlinear normality versus nonnormal linearity. *Phys. Fluids* 7: 3060–3066

Wall D P, Wilson S K 1996 The linear stability of channel flow of fluid with temperature-dependent viscosity. *J. Fluid Mech.* 323: 107–132